Title

A Multi-Fluorophore Staining Scheme for Identification and Quantification of Vomocytosis

Journal

Chemical & Biomedical Imaging, 1(8)

ISSN

2832-3637

Authors

Pacifici, Noah
Rojalin, Tatu
Carney, Randy P
et al.

Publication Date

2023-11-27

DOI

10.1021/cbmi.3c00050

Peer reviewed

ACS Partner Journal

CHEMICAL & BIOMEDICAL IMAGING

pubs.acs.org/ChemBioImaging

Article

A Multi-Fluorophore Staining Scheme for Identification and Quantification of Vomocytosis

Noah Pacifici, Tatu Rojalin, Randy P. Carney, and Jamal S. Lewis*

Cite This: *Chem. Biomed. Imaging* 2023, 1, 725−737

Read Online

ACCESS | Metrics & More | Article Recommendations | Supporting Information

ABSTRACT: Vomocytosis is a process by which fungal pathogens, for instance, *Cryptococcus neoformans* (CN), escape from the digestive phagolysosome of phagocytic cells after ingestion. Interestingly, this expulsion leaves both the pathogen and phagocyte unharmed, and is believed to be an important mechanism by which CNs disseminate throughout infected hosts. This phenomenon was discovered in 2006, and research to date has relied almost entirely on quantification via manual counting of vomocytosis events in time-lapse microscopy videos. This archaic method has the significant disadvantages of requiring excessive labor in manual analysis, limited throughput capabilities, and low accuracy due to subjectivity. Here, we present an alternative method to measure vomocytosis rates using a multi-fluorophore reporter system comprised of two *in situ* staining steps during infection and a flow cytometry readout. This approach overcomes the limitations of conventional time lapse microscopy methods, with key advantages of high throughput capability, simple procedural steps, and accurate objective readouts. This study rigorously characterizes this vomocytosis reporter system in CN-infected MΦ and DC cultures via fluorescence microscopy, confocal microscopy, and flow cytometry. Here, this fluorescent tool is used to observe differences in expulsion rates after phagosome-modifying drug treatments and additionally utilized to distinguish differences in biochemical compositions among fluorescence-activated cell sorted fungal populations via Raman spectroscopy. Furthermore, this reporter scheme is demonstrated to be adaptable for use in measuring potential biomaterial particle expulsion events. Ultimately, the fluorescent reporter system presented here provides a universal tool for vomocytosis rate measurement of phagocytosed material. This facile approach opens the door to previously unfeasible types of vomocytosis-related studies such as high throughput treatment mechanistic screening and downstream characterization of expelled material.

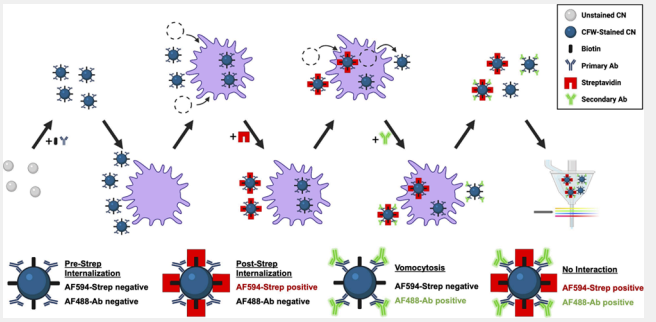

KEYWORDS: *Vomocytosis, Macrophages, Dendritic cells, Detection, Quantification, Isolation, Raman spectroscopy*

1. INTRODUCTION

Pathogens have evolved over time to evade the host immune system in various ways. The fungal species, *Cryptococcus neoformans* (CN), is equipped with numerous mechanisms to resist and avoid the innate immune system. One primary example is CN's ability to persist within the acidic phagolysosome after engulfment by phagocytes and escape through a process called vomocytosis (nonlytic exocytosis), which leaves the host and pathogen cells unharmed.[1−4] This unique attribute is highly relevant to mechanisms of fungal dissemination within infected hosts. After entering a host via inhalation, these fungal cells first encounter alveolar macrophages (MΦs) within the lungs that ingest the invading CN. However, rather than digesting and killing the pathogens, these immune cells are hijacked to act as a shuttle to transport infection throughout the body. This is possible due to the ability of CN to survive within the digestive phagosome and trigger vomocytic escape after several hours.[5] Through this "Trojan Horse" mechanism of dissemination, infection can even cross the highly guarded, blood brain barrier into the central nervous system of the host and may result in a condition called cryptococcal meningitis (CM). Primarily affecting immunocompromised individuals, including an estimated 220,000 HIV/AIDS patients, CM causes ∼181,000 deaths/year worldwide.[6] Crucially, greater understanding of vomocytosis could lead to the development of new CM treatments for patients.

Due to the relevance of MΦs in CM infections, vomocytosis studies thus far have primarily focused on the occurrence of this event in this one cell type. However, other phagocytic cell types—neutrophils[7] and dendritic cells[8] (DCs)—have recently

Received: May 22, 2023
Revised: July 24, 2023
Accepted: July 26, 2023
Published: August 8, 2023

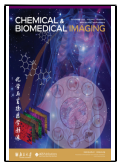

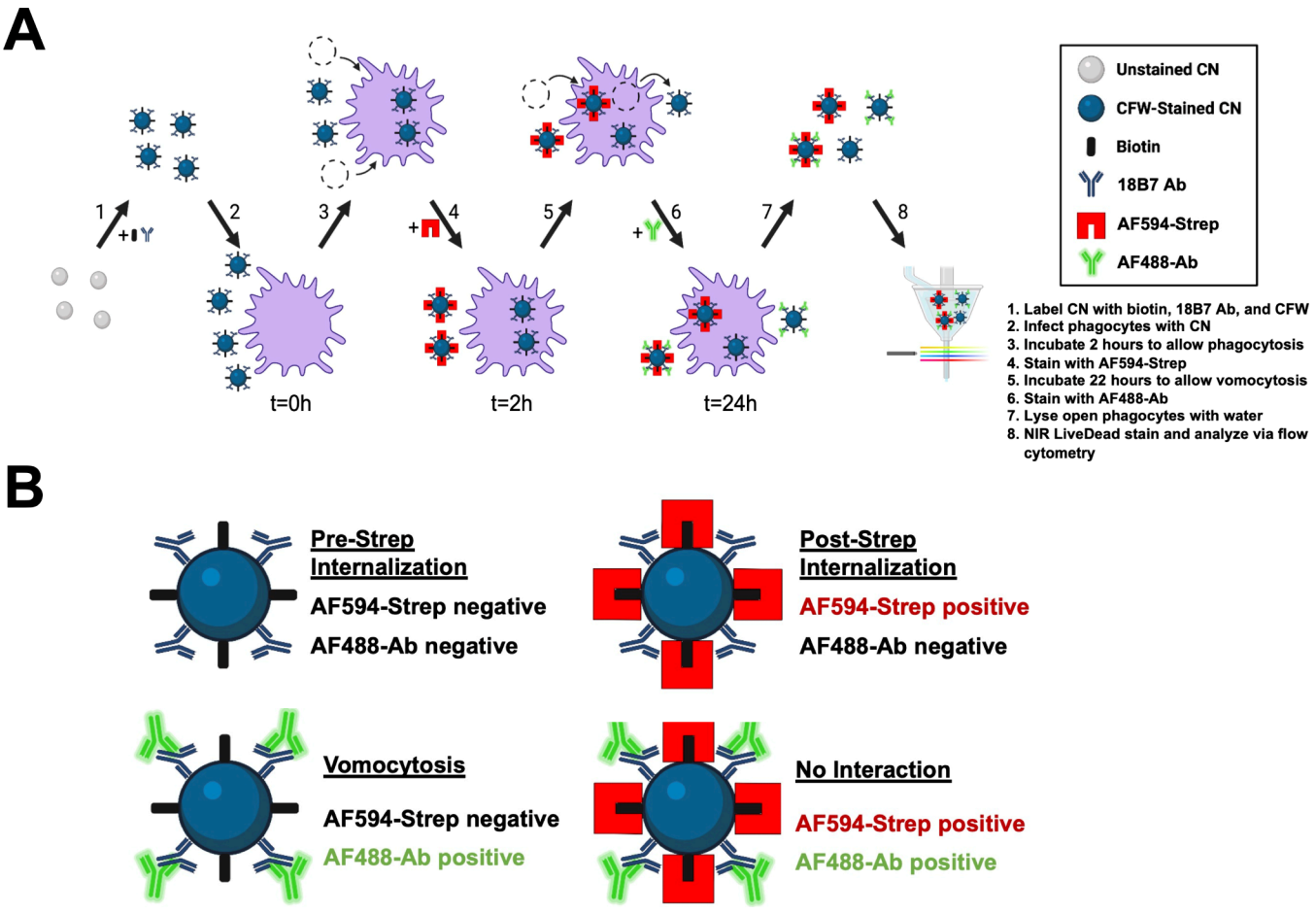

Figure 1. Schematic illustrating the design of the vomocytosis reporter system. (A) The experimental steps of the reporter system consist of (1) conjugating biotin to CN via NHS chemistry, opsonizing with 18B7 Ab, and labeling with CFW fungal stain; (2) infect CN with phagocytes at a 2:1 CN:phagocyte ratio; (3) incubate for 2 h to allow for phagocytosis of CN; (4) apply AF594-Strep to culture to stain only extracellular CN at this time point and confirm internalization; (5) incubate for 22 more hours to allow for vomocytosis events to occur; (6) apply AF488-Ab to culture to stain only extracellular CN at this time point and confirm expulsion; (7) lyse open phagocytes using sterile water to release any internalized CN; (8) apply NIR LiveDead stain on CN to identify and remove nonlive fungal cells, and run flow cytometry analysis of CN fluorescence. (B) Based primarily on the two key reporter fluorescent stains of AF594-Strep and AF488-Ab, there are four different scenarios for CN outcome of incubation with phagocytes. Either double negative (phagocytosed prior to AF594-Strep stain, and remains internalized: "pre-strep internalization"), single positive AF594-Strep (phagocytosed after AF594-Strep stain, and remains internalized: "post-strep internalization"), single positive AF488-Ab (vomocytosed), and double positive (no interaction with phagocytes during experiment).

been documented to perform vomocytosis of CN during infection. However, the underlying mechanisms of this phenomenon are mostly unknown, with only a small handful of phagosomal properties, proteins, and immunological phenotypes known to affect expulsion rates.[3,4] Moreover, in the published literature there is much disagreement, which likely stems from the lack of an objective tool to measure vomocytosis.

To efficiently study vomocytosis, a robust method for quantifying phagocytosis and expulsion rates is needed. However, there is currently a deficiency in availability of effective techniques for measuring the occurrence of these expulsion events. Present studies rely primarily on manual counting of vomocytic events via time lapse microscopy of unstained or fluorescently stained phagocyte infections with CN. While straightforward, time lapse microscopy quantification of vomocytosis is a highly time-consuming and labor-intensive option, as hundreds of hours of cell culture footage must be stored and analyzed manually for just a limited number of data replicates. Another limitation of this technique is the necessity for access to or ownership of expensive time lapse microscopy and in-stage cell incubation equipment. Lastly, a crucial drawback of time lapse microscopy is that video analysis is highly subjective; even when analyzed in a blinded manner, the accuracy of such measurements is highly unreliable, especially when attempting to distinguish marginal differences in vomocytosis rates between treatment groups. For instance, one study found that manual time lapse analysis of cell migration had a miscalculation rate of up to 410%.[9]

Apart from time lapse microcopy, there is another method developed by Nicola et al. that uses a fluorescence-activated cell sorting (FACS)-centered approach for detecting expulsion of CN from phagocytes.[10] The process involves staining and FACS to isolate live phagocytes with internalized CNs, then incubating this subpopulation for a given period, and analyzing via flow cytometry at the end point to determine which intact phagocytes no longer contain CN. The approach has advantages over time lapse microscopy in allowing for objective quantification of expulsion in a systematic manner, and has been used in multiple studies to measure vomocytosis

https://doi.org/10.1021/cbmi.3c00050
Chem. Biomed. Imaging 2023, 1, 725−737

rates.[7,10−12] However, this method also displays significant limitations. In a similar drawback to time lapse microscopy, the Nicola et al. protocol requires use of expensive FACS equipment, which may not be available or accessible to most laboratories. This cell-sorting step is performed midexperiment and may influence cell behavior. Importantly, another key limitation of this staining protocol is its narrow applicability, only being compatible with capsular fungal cells such as CN. The technique does not have the capability to measure expulsion rates of other microbes or nonbiological particulates due to its required use of the fungal extracellular stain, Uvitex 2B, which is only applicable for fungal cells. In its current state, the field of vomocytosis research needs new methodologies for quantifying expulsions that can overcome the long-standing limitations of conventional approaches.

This study outlines a novel, simple, multifluorescent staining scheme that enables precise monitoring of phagocytic entry and vomocytic expulsion of CN from phagocytes during infection. This system is composed of a prelabeling step of CN followed by two extracellular stains during infection, and finally flow cytometry analysis of stained CN (Figure 1A). Prior to infection, CNs are coated with biotin using *N*-hydroxysuccinimide (NHS) chemistry. Additionally, CNs are pre-labeled with a fungal tracking dye Calcofluor White (CFW) and opsonized with an anticapsule 18B7 antibody (18B7 Ab). After a 2 h phagosomal ingestion incubation period, a fluorescent AlexaFluor (AF) 594-conjugate of streptavidin (AF594-Strep) is applied to target biotin on the surface of external CN located outside of the phagosome. This step is used to distinguish phagocytosed from nonphagocytosed CN at this time point. Next, at an ending time point of 24 h after initial infection, any external CNs are stained using a fluorescent AF488 secondary antibody (AF488-Ab) targeting the 18B7 Ab present on the surface of external CN. This second stain is used to determine which CNs have been vomocytosed. While some CNs may enter and exit during this period, those cases are minimized by removing the opsonizing 18B7 Ab after the phagocytosis period to reduce further internalization. These selective extracellular stains are achievable due to the bulky nature of AF594-Strep and AF488-Ab. Finally, for the purpose of qualifying this system, phagocytes are lysed via sterile water to free any internalized CNs, and a Near-IR Dead Cell Stain Kit (NIR LiveDead) is applied to identify between live and killed fungal cells. Through assessing each fungal cell via flow cytometry, the fluorescence of these two key reporter stains (AF594-Strep and AF488-Ab) are able to distinguish between the four outcome scenarios of CN after incubation with phagocytes: (i) phagocytosis prior to AF594-Strep labeling: "pre-strep internalization"; (ii) phagocytosis after AF594-Strep labeling: "post-strep internalization"; (iii) phagocytosis prior to AF594-Strep labeling, then expulsion, and labeling with AF488-Ab: "vomocytosis", and (iv) remaining extracellular for both AF594-Strep and AF488-Ab labeling: "no interaction" (Figure 1B). In this study, the functionalities of the reporter system components are demonstrated through widefield fluorescence microscopy and then validated by flow cytometry and confocal microscopy. Subsequently, the full reporter staining protocol is used to detect real vomocytosis rates of CN after incubation with either MΦs or DCs. The reporter system is shown to also distinguish differences in vomocytosis occurrence of CN-infected cultures treated with drugs that modify the phagosomal physicochemical environment and actin polymerization. Furthermore, single cell Raman spectroscopy of FACS-sorted reporter-stained CN cells is used to confirm that these fungal populations have distinct biochemical compositions depending on the outcome of phagocyte interaction for infections with either MΦs or DCs. Finally, the reporter system protocol is adapted to detect "pseudoexpulsion" rates of poly(lactic-*co*-glycolic) (PLGA) microparticles (MPs) phagocyted by MΦs or DCs to demonstrate the flexibility of this universal system to objectively quantify phagocytic expulsion of both pathogenic fungi and biomaterial particles. This high throughput tool allows for facile identification and quantification of vomocytosis, which importantly aids studies for host−pathogen mechanistic research and novel therapeutic development.

2. MATERIALS AND METHODS

Bone Marrow-Derived MΦ and DC Culture

Phagocytes were grown via differentiating bone marrow progenitor cells from 8 to 12 week old C57BL/6 mice as described in previous studies.[13] Cell media used was DMEM/F-12 1:1 with L-glutamine (Cellgro, Herndon, VA) and contained 10% fetal bovine serum (R&D Systems, Minneapolis, MN), 1% nonessential amino acids (Lonza, Walkersville, MD), 1% sodium pyruvate (Lonza), 1% penicillin/streptomycin (Cytiva, Marlborough, MA), and a differentiation factor. For MΦ media, the differentiation factor was M-CSF supplied by 20% L929-treated media. The differentiation factor for DC media was 20 ng/mL GM-CSF (R&D Systems). Cells were plated on day 6 of culture and used for experiments between days 8−12.

Cryptococcus neoformans Culture

A *Cdc24* mutant strain of CN (generously gifted by Dr. Angie Gelli, UC Davis, CA) was used for the entirety of this study due to its lack of replication at 37 °C.[14] Prior to infection, CNs were grown first by streaking a frozen culture on yeast peptone dextrose (YPD) agar (Thermo Fisher Scientific, Waltham, MA) at 30 °C. Once visible colonies formed, a single colony of CN was transferred to YPD broth (Thermo Fisher Scientific) and left shaking overnight at 30 °C.

Pre-Labeling of CN for Reporter Staining

Before infection or reporter staining, CNs were first labeled with biotin. Biotin was conjugated to the surface of the fungal cells using NHS chemistry. Briefly, 1×10^6 CN/mL was incubated with 2 mg/mL NHS-dPEG12-biotin (Sigma, St. Louis, MO) for 45 min. After this labeling, excess reagent was washed 3 times with PBS via centrifugation. Next, CN was stained with a fluorescently active fungal dye CFW (Sigma) at a concentration of 1 mg/mL for 15 min and then washed 3 times using 1% w/v of bovine serum albumin (BSA, Sigma) in PBS (hereby referred to as "protein buffer") via centrifugation. Finally, the fungal cells were coated with 10 μg/mL of anticapsular 18B7 Ab (supplied from both Sigma and the Casadevall Lab, Johns Hopkins University, MD) for 30 min. For brevity, CNs labeled with biotin, CFW, and 18B7 Ab are simply referred to as "pre-labeled CN".

Fluorescence Microscopy of Reporter-Stained CN Infections

Fluorescence microscopy was utilized for visual assessment of CN reporter staining. Macrophages were seeded onto a 12-well culture plate at a density of 1×10^5 cells/well. Next, the phagocytes were infected with pre-labeled CN at a 2:1 CN:phagocyte ratio for 2 h and then rinsed 3 times with warm PBS. Reporter stains of either 5 μg/mL AF594-Strep (Biolegend, San Diego, CA) or 10 μg/mL AF488-Ab (polyclonal goat antimouse IgG, Thermo Fisher Scientific) were applied to the adherent infected culture for 30 min in protein buffer. Cells were then gently rinsed with warm PBS 3 times and imaged using a BZ-X Fluorescence Microscope (Keyence, Itasca, IL) for a CFW fluorescence (DAPI filter cube, Keyence), AF594-Strep signal (TxRed filter cube, Keyence), and AF488-Ab signal (GFP filter cube, Keyence).

https://doi.org/10.1021/cbmi.3c00050
Chem. Biomed. Imaging 2023, 1, 725−737

Confocal Fluorescence Microscopy of Reporter-Stained CN Infections

Reporter staining was also assessed via confocal microscopy for z-stack localization of CN. Prior to infection, MΦs were stained with 1 μM of 1,1′-dioctadecyl-3,3,3′,3′-tetramethylindodicarbocyanine, 4-chlorobenzenesulfonate salt (DiD; Thermo Fisher Scientific) as a lipophilic dye tracer, and seeded onto a glass chamber slide. Phagocytes were infected 2:1 phagocyte:CN with pre-labeled CN. After a 2 h incubation to allow for phagocytosis, the culture was rinsed 3 times with PBS and stained with either 5 μg/mL AF594-Strep or 10 μg/mL AF488-Ab in protein buffer. After 3 additional washes, cells were fixed with 2% paraformaldehyde diluted with PBS and imaged using the Olympus FV3000 confocal (Olympus Corporation, Westborough, MA) at 60× magnification. For each condition, 50 confocal image slices of 300 nm thickness were acquired and then used to create 3D volume renders and combined z-stack images.

Reporter System Measurement of CN Vomocytosis Events Via Flow Cytometry

To validate the performance of the reporter system, CN-infected phagocyte cultures were assessed for vomocytosis occurrence. First, adherent phagocytes (MΦs or DCs) that were grown on a 6-well culture plate at ∼1 × 10^6 cells per well were lifted into suspension via incubation with warm PBS with 2.5 mM ethylenediaminetetraacetic acid (EDTA) and 2.5 mM dextrose and then scraped after 10 min. Macrophages or DCs in media were infected with pre-labeled CN at a 2:1 CN:phagocyte ratio while in suspension; these cultures were kept within individual tubes and incubated at 37 °C with lids open while loosely covered with aluminum foil to allow air exchange. After 2 h to allow for phagocytosis, the cultures were rinsed once with protein buffer via centrifugation. The cultures were then stained with AF594-Strep at a 5 μg/mL concentration for 30 min, rinsed with protein buffer, and resuspended in warm fresh media. After 22 h, or 24 h after phagocytosis, 10 μg/mL fluorescent AF488-Ab was applied to the infected cultures for 30 min and subsequently rinsed with protein buffer. Next, the phagocytes within the tubes were lysed via incubation in cold sterile water for 30 min. To assess the viability of the CN, a Near-IR Dead Cell Stain Kit (NIR LiveDead, Thermo Fisher Scientific) was applied according to the manufacturer's instructions. The LiveDead selectively labels dead cells by staining the intracellular proteins of those cells with compromised membranes. Finally, the stained CNs were fluorescently analyzed via flow cytometry on an Attune NxT Flow Cytometer (Thermo Fisher Scientific). Refrigerated controls were treated identically to Live CN-infected groups, except after AF594-Strep staining the cultures were kept at 4 °C for the remainder of the experiment. For heat-killed (HK) CN controls, CNs were placed in a heat block at 70 °C for 1 h prior to labeling and infection. The methods are otherwise identical to that of live CN. For flow cytometry analysis, vomocytosis events were categorized as CFW positive, AF594-Strep negative, and AF488-Ab positive, with dead cell events removed from the final statistic (NIR LiveDead positive cells removed). Vomocytosis percentage was calculated by dividing the vomocytosis events by the phagocytosed population (CFW positive and AF594-Strep negative events).

Flow Cytometry Evaluation of Phagocyte Viability after CN Infection

To assess the viability of phagocytes during infection conditions, DCs or MΦs were first stained with 1 μM DiD as a tracking label. Then the phagocytes were either left uninfected or were infected with live or HK CN at a 2:1 CN:phagocyte ratio (2 × 10^5 CN, 1 × 10^5 phagocytes) for 24 h in suspension. The cells were then stained with propidium iodide (PI; Sigma) at a concentration of 2 μg/mL in 0.1% BSA in PBS buffer for 30 min. Via flow cytometry, phagocyte viability was assessed by first gating on DiD-positive cells and then assessing the percent positive gated for PI (dead) signal.

Measurement of Vomocytosis Rates Using the Reporter System for Drug-Treated Phagocyte Cultures Infected with CN

The reporter staining procedure for drug-treated experimental groups was identical to non-drug-treated groups as outlined previously. For drug-treated groups, the phagocytes were first infected with CN in drug-free media. However, after AF594-Strep staining, these groups were then incubated with the relevant drug-containing media for the remainder of the infection. Cells were treated with 100 nM bafilomycin A1 (BFA, Sigma), 4 μM cytochalasin B (CYT hi, Sigma), 100 nM cytochalasin B (CYT lo), or 10 μM chloroquine (CQ, Thermo Fisher Scientific). These drugs and their concentrations were selected based on relevant reference experiments from vomocytosis studies.[7,8,10,15,16]

Reporter-Stained CN FACS Sorting and Post-Sort Purity Analysis

Prior to FACS sorting, phagocytes (MΦs or DCs) were infected with live pre-labeled CN in suspension as previously outlined. Throughout the 24 h infection, the culture was stained with the reporter components, lysed to liberate intracellular CN, and NIR LiveDead stained using identical methods outlined for prior reporter experiments. The resulting stained CN was kept on ice and sorted using an Astrios EQ (Beckman Coulter, Brea, CA) by the UC Davis Flow Core. Events were first gated for positive CFW and negative NIR LiveDead signal and then sorted by AF594-Strep and AF488-Ab signal into 4 separate tubes with a minimum of 1000 events each for both MΦ and DC (8 sorted tubes total). Small allocations of each sorted sample were then run on the Attune NxT Flow Cytometer to assess post-sort purity, again gated on positive CFW and negative LiveDead.

Single Cell Laser Trapping Raman Spectroscopy (LTRS) Analysis of Reported-Sorted CN during Infection

The LTRS spectra were acquired using a custom-built inverted Raman scanning confocal microscope with an excitation wavelength of 785 nm and a 60×, 1.2 NA water immersion objective on an inverted IX73 Olympus microscope. Raman spectra were recorded via an Andor Kymera-3281-C spectrophotometer and Newton DU920P-BR-DD CCD camera. Preliminary *in situ* data processing was performed using Solis v4.31.30005.0 software. The physical working principle of LTRS is based on using a tightly focused laser beam to form an optical trap.[17−19] The same beam is also used to excite Raman scattering from the irradiated samples of interest in the trap. This approach enables highly sensitive chemical fingerprinting of single optically trapped particles, such as CN, in native aqueous environments. The laser exposure time was set to 60 s per scan (i.e., one single trapped cell was measured for 60 s), with a laser power of ∼65 mW, and pinhole aperture set to 1 mm (epi-mode). At least 10 individual spectra were collected per each sample type (total 8 sample types). The post-collection spectra analysis was performed using custom scripts written in MATLAB v2021b (MathWorks, MA, USA). Spectral post-collection included cosmic ray removal, penalized least-squares (PLS) background correction, smoothing, and normalization. The spectra were cropped to the biological spectral fingerprint region of ∼800−1800 cm^{-1}. Subsequently, the processed spectral sets were subjected to principal component analysis (PCA) and hierarchical clustering analysis based on the corresponding MATLAB built-in functions.[20,21] The custom MATLAB scripts and the associated in-house spectra processing software can be provided upon request.

Fabrication and Preparation of PLGA MPs for Reporter System Experiments

Phagocytosable PLGA MPs were created using an oil-in-water emulsion using a Tissuemiser homogenizer (OMNI, Kennesaw, GA) as described in previous studies.[13] A 1:1 blend of acid-terminated PLGA (PURASORB PDLG 5004A from Corbion, Amsterdam, Netherlands) and 8-arm PLGA-Azide (Nanosoft Polymers, Winston-Salem, NC) were used, both with 50:50 lactic-to-glycolic acid ratio and 20 kDa molecular weight parameters.

https://doi.org/10.1021/cbmi.3c00050
Chem. Biomed. Imaging 2023, 1, 725−737

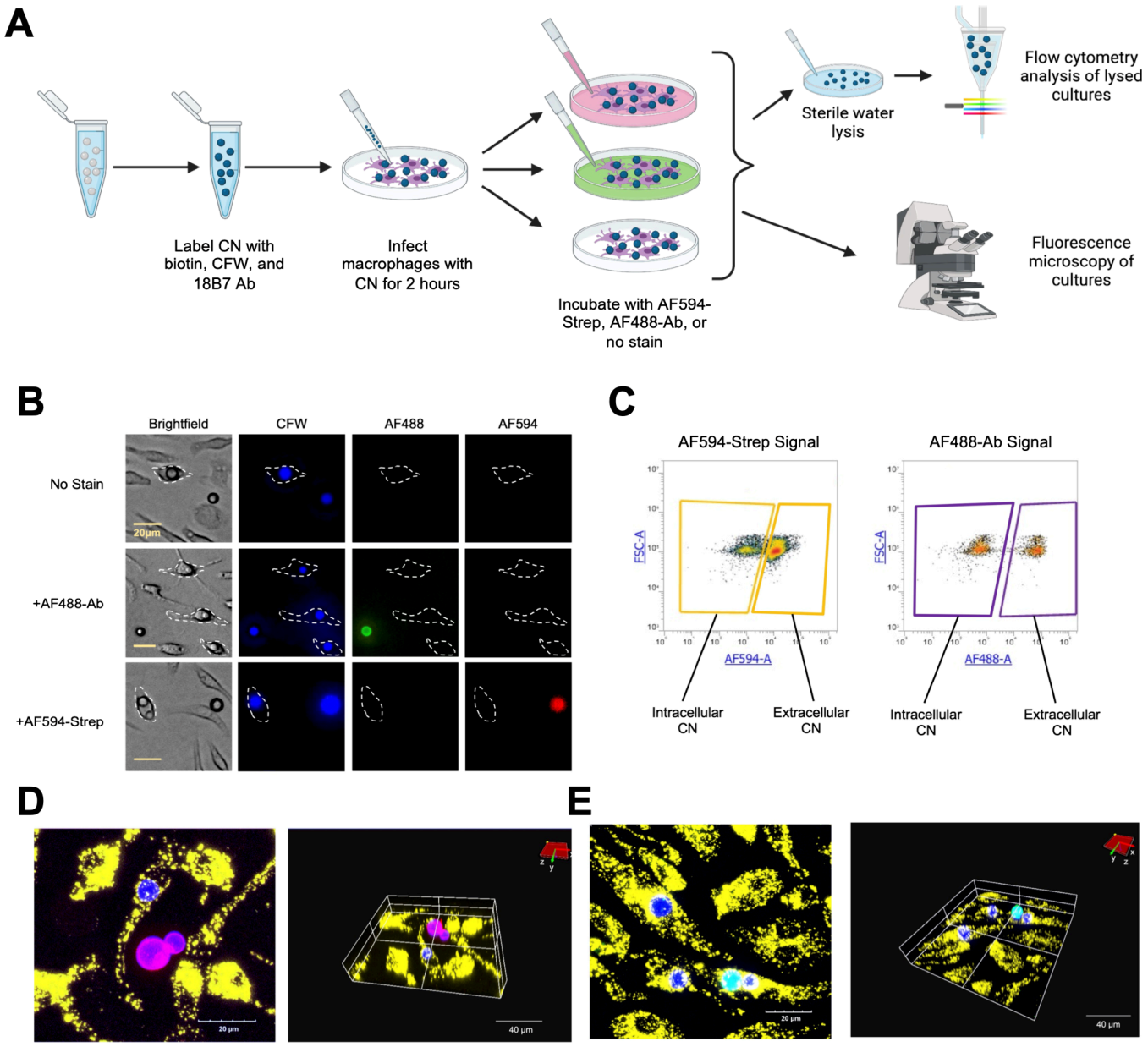

Figure 2. AF594-Strep and AF488-Ab extracellular staining ability confirmed via fluorescent microscopy, flow cytometry, and confocal microscopy. (A) Schematic of experimental design. Prior to infection, CN was labeled with biotin, CFW, and 18B7 Ab. Then MΦs were infected with labeled CN and incubated for 2 h. Cultures were then stained with AF594-Strep, AF488-Ab, or no stain and analyzed via microscopy or flow cytometry. (B) Fluorescence microscopy confirmation of extracellular staining. Pre-staining of CFW in blue is shown for all CNs in the images. When AF488-Ab stain was applied, any extracellular CN was stained with green AF488 fluorescence. If incubated with the AF594-Strep stain, cultures displayed a red AF594 fluorescence signal only on extracellular CN. Both stains leave internalized CN unstained. (C) Flow cytometry confirmation of extracellular staining. After either AF594-Strep or AF488-Ab staining, both lysed cultures displayed distinct gate-able flow cytometry populations by the respective fluorescence signal. (D) Confocal confirmation of AF594-Strep extracellular staining via a combined Z stack (left) and 3D volume render (right). In the images, stains are shown for MΦ (DiD, yellow), CN (CFW, blue), and AF594-Strep (AF594, red). As visualized in the images, only the extracellular CN was stained by AF594-Strep. (E) Confocal confirmation of AF488-Strep extracellular staining via a combined Z stack (left) and 3D volume render (right). Stains are shown for MΦ (DiD, yellow), CN (CFW, blue), and AF488-Ab (AF488, green).

To functionalize the PLGA MPs for reporter experiments, the particles were first conjugated with biotin using click chemistry via incubation with 100 μM Biotin-dPEG12-DBCO (Sigma) for 30 min. The MPs were then washed with PBS and stained with FITC, again utilizing click chemistry via incubation with 100 μM DBCO-PEG2000-fluorescein (Nanocs, New York, NY) for 30 min. Finally, the functionalized PLGA MPs were rinsed with protein buffer via centrifugation to remove remaining reagents. For conciseness, these PLGA MPs with conjugated biotin and FITC are hereby referred to as "pre-labeled PLGA MPs".

Fluorescence Microscopy Visualization of Reporter-Stained PLGA MP after Phagocytosis by MΦs

For fluorescence microscopy experiments, MΦs were seeded onto a 12-well plate at a density of 1×10^5 cells per well. Then pre-labeled PLGA MPs were incubated with the MΦs at a 10:1 MP:phagocyte ratio. After a 1 h phagocytosis period, excess MPs were washed off via rinsing with PBS (3 times). Cultures were either left unstained, stained with 5 μg/mL AF594-Strep, or stained with 20 μg/mL allophycocyanin (APC) conjugate of anti-FITC antibody (APC-Ab, FIT-22 Mouse Clone, Biolegend) in protein buffer for 30 min. Excess

https://doi.org/10.1021/cbmi.3c00050
Chem. Biomed. Imaging 2023, 1, 725−737

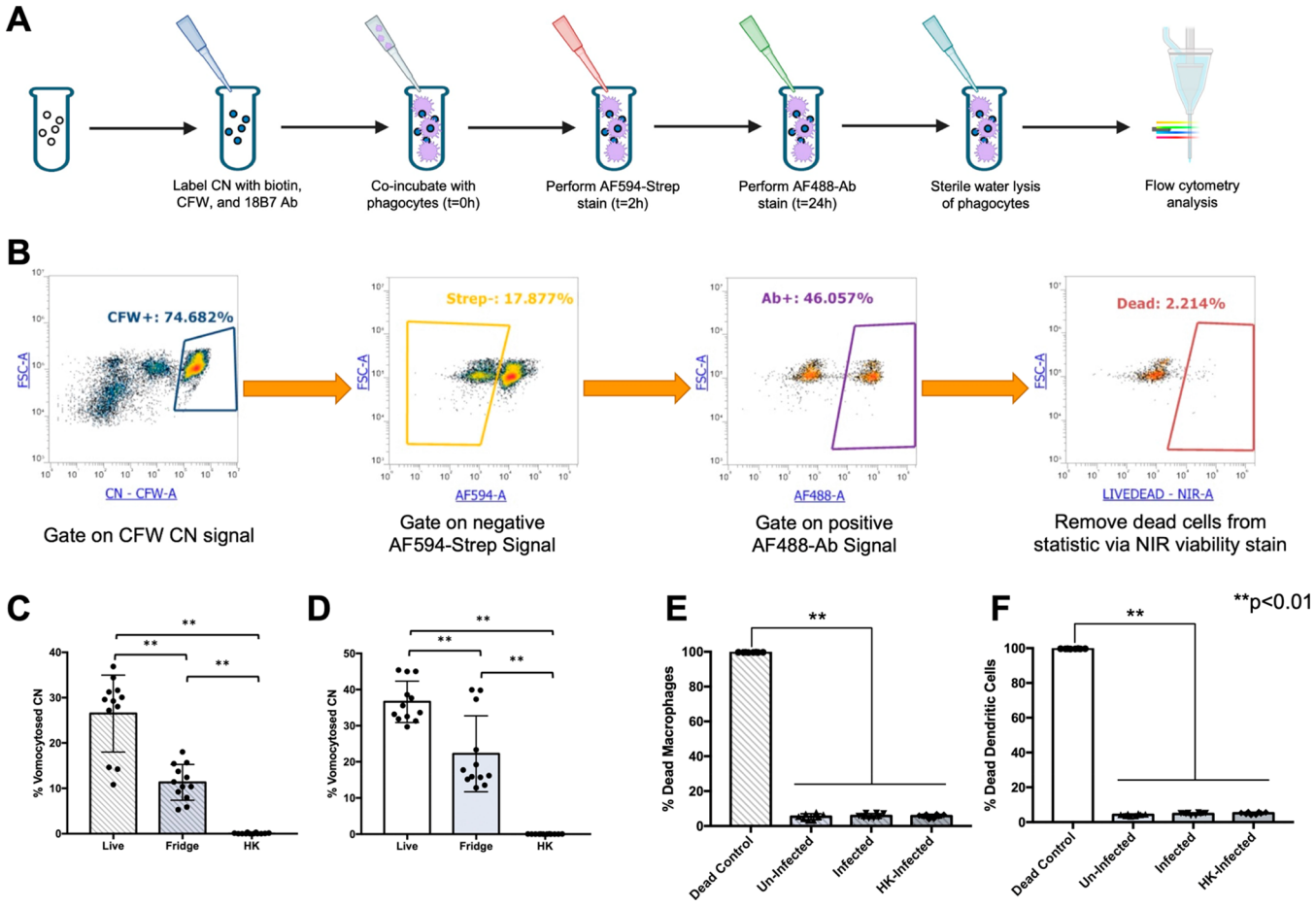

Figure 3. Reporter system capability to measure vomocytosis rates of MΦs and DCs. (A) Schematic of experimental design for reporter system staining. First, CN was coated with biotin, CFW, and 18B7 Ab. The fungal cells were next incubated with phagocytes (MΦ or DC) at 2:1 CN:phagocyte for 2 h to allow for phagocytosis. During the infection, the culture was stained with AF594-Strep at t = 2 h and AF488-Ab at t = 24 h. Then the cultures were lysed using sterile water and analyzed for fluorescence via flow cytometry. (B) Gating process for the analysis of flow cytometry data. First, only CFW positive events were gated to select CN from debris. Next, negative AF594-Strep signal events were gated to select only CN that was internalized at t = 2 h. From this population, positive AF488-Ab signal events were gating to measure the percentage of internalized CN that was expelled. Finally, NIR LiveDead signal was used to assess the viability of the exocytosed CN to remove unviable cells from the final vomocytosis rate calculation. (C) Bar graph of reporter-measured CN vomocytosis rates during MΦ infection. Macrophages were infected with live CN or HK CN. Additionally, a refrigerated control was used to slow vomocytosis rates at 4 °C during the incubation after AF594-Strep staining (N = 4, n = 12). (D) Bar graph of reporter-measured CN vomocytosis rates during DC infection. Live CN vomocytosis rates were compared to HK CN and refrigerated controls (N = 4, n = 12). (E) Bar graph of MΦ viability after CN infection. The viability of uninfected, live-infected, and HK-infected MΦs was assessed via PI staining and compared to a MΦ heat-treated control (N = 3, n = 9). (F) Bar graph of DC viability after CN infection. The viability of uninfected, live-infected, and HK-infected MΦs were assessed via PI staining and compared to a MΦ heat-treated control (N = 3, n = 9). All statistical analyses were one-way ANOVAs corrected for multiple comparisons by a false discovery rate (FDR) using a two-stage linear step-up procedure of Benjamini, Krieger and Yekutieli via GraphPad Prism 9.

dye was rinsed off using protein buffer, and the *in vitro* cultures were imaged using a BZ-X Fluorescence Microscope for FITC fluorescence (GFP filter cube), AF594-Strep signal (TxRed filter cube), and APC-Ab signal (Cy5 filter cube, Keyence).

Reporter Staining and Flow Cytometry Measurement of PLGA MP Pseudo Vomocytosis Rates after Incubation with Phagocytes

Pre-labeled PLGA MPs were incubated with MΦs or DCs at a 5:1 MP:phagocyte ratio for 1 h in suspension to allow for phagocytosis. The resulting cultures were then stained with 5 μg/mL AF594-Strep for 30 min. Next, one group was split into two tubes, one of which was treated with sterile water for lysis and the other left unlysed; then the two tubes were recombined, and together this was called the "partial lysis" condition. Next, the culture was stained with 20 μg/mL APC-Ab for 30 min as an extracellular stain for the FITC tracker on the surface of the PLGA MPs. For the unlysed control, the culture was stained with APC-Ab without prior lysis. After this stain, the groups were then fully lysed by sterile water, rinsed with protein buffer, and analyzed via flow cytometry. Vomocytosis events were categorized as FITC positive, AF594-Strep negative, and APC-Ab positive. Vomocytosis fraction (percentage; ×100) was calculated by dividing the vomocytosis events by the phagocytosed population (events positive for FITC and negative for AF594-Strep).

Data and Statistical Analysis

Statistical analyses were performed using GraphPad Prism 9. Comparisons between reporter-measured vomocytosis rates were evaluated via one-way ANOVA corrected for multiple comparisons by the false discovery rate (FDR) using a two-stage linear step-up procedure of Benjamini, Krieger, and Yekutieli. The normality of sample groups was assessed using a D'Agostino and Pearson normality test (α = 0.05). All statistical analyses were performed on GraphPad Prism 9. The same statistical methods were also used to compare the viability of phagocytes under different infection conditions. For experiments comparing reporter measurements of

https://doi.org/10.1021/cbmi.3c00050
Chem. Biomed. Imaging 2023, 1, 725−737

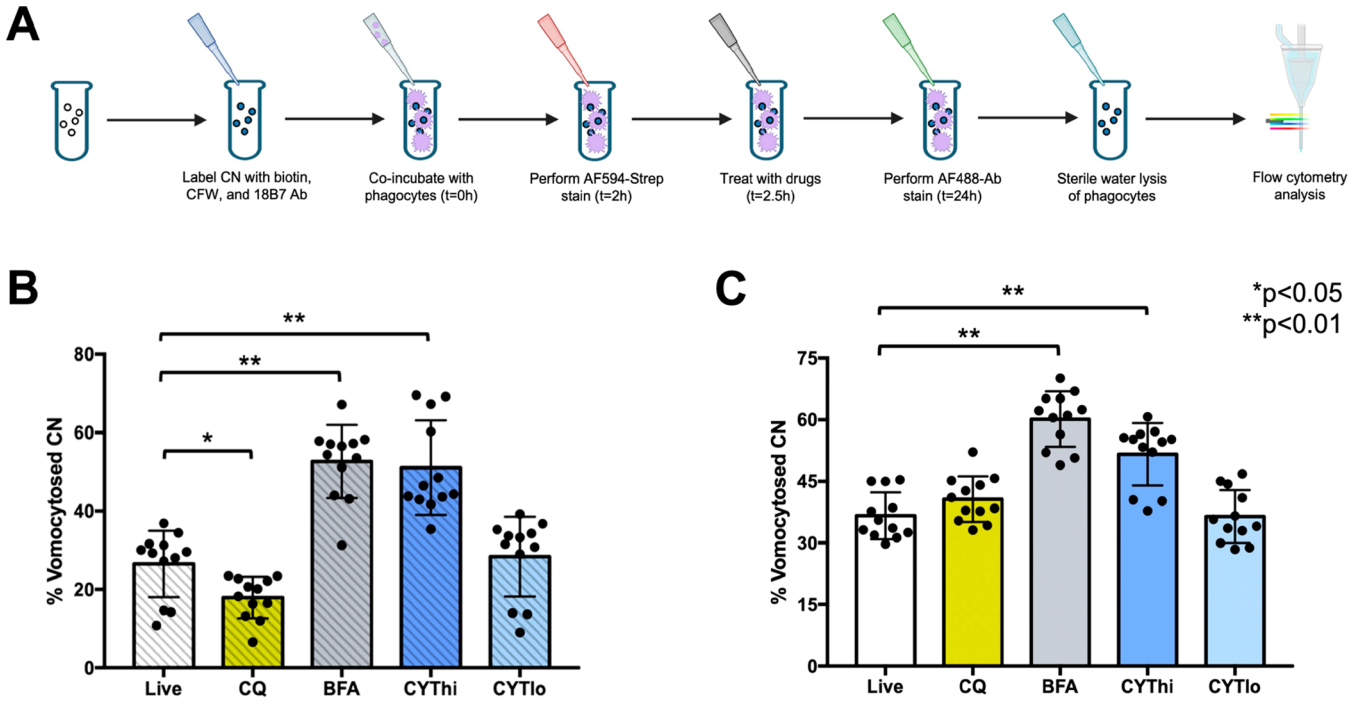

Figure 4. Reporter system used to measure differences in vomocytosis rates of phagocytes treated with phagosomal- or actin-modifying drugs. (A) Schematic outlining the experimental design for drug-treated reporter system vomocytosis quantification. Briefly, CN was pre-labeled with biotin, CFW, and primary Ab and then incubated with phagocytes (MΦ or DC) for 2 h. The AF594-Strep stain was then performed, followed by drug treatment. At the end time point of 24 h, AF488-Ab staining was performed. Subsequently, phagocytes were lysed, and CN was analyzed via flow cytometry for vomocytosis rate assessment. (B) Bar graph of vomocytosis rates of CN during drug-treated MΦ infections. Macrophages infected with live CN were treated with CQ, BFA, CYT hi, or CYT lo drug incubations after phagocytosis, and the vomocytosis rates of CN were measured using the reporter system (N = 4, n = 12). (C) Bar graph of vomocytosis rates of CN during drug-treated DC infections. Dendritic cells were infected with live CN and then treated with CQ, BFA, CYT hi, or CYT lo drug incubations after phagocytosis. Vomocytosis rates of CN were subsequently measured via the reporter system (N = 4, n = 12). All statistical analyses were one-way ANOVAs corrected for multiple comparisons by false discovery rate (FDR) using a two-stage linear step-up procedure of Benjamini, Krieger and Yekutieli via GraphPad Prism 9.

PLGA MP expulsion from phagocytes, an unpaired t test was used as there were only two groups (unlysed and partial lysis) to compare. All data shown include at least three independent experiments with phagocytes sourced from the bone marrow of separate mice. Categorical data were converted to continuous data via sample replicates being documented as percentage values. All column graphs, generated on GraphPad Prism 9, display the individual data points, mean, and standard deviation (SD). A summary of all statistical tests and p-values are listed in Table S1.

3. RESULTS AND DISCUSSION

AF594-Strep and AF488-Ab Reporter Components Selectively Stain Extracellular CN during *In Vitro* Phagocyte Infection

For the reporter system to function as designed, the AF594-Strep and AF488-Ab stains must selectively stain only extracellular CN during infection. To investigate the performance of the reporter stains, MΦs were infected with pre-labeled CN and stained with AF594-Strep or AF488-Ab after phagocytosis and then analyzed via fluorescence microscopy and flow cytometry (Figure 2A). Through fluorescence imaging, AF488-Ab (green) and AF594-Strep (red) labeling of CNs (blue) shows the selectivity of each stain for extracellular CN only, while phagocytosed CN remains unstained (Figure 2B). Additionally, after lysis of reporter-stained cultures, flow cytometry analysis of AF594-Strep and AF488-Ab signal can be used to create gates for internalized or externalized CN (Figure 2C). Additionally, through confocal imaging of fixed cultures after reporter staining, the selectivity of each stain for external CN can be clearly visualized for both AF594-Strep and AF488-Ab signal (Figure 2D,E). These results indicate that the reporter system components perform as expected with high signal resolution to be distinguishable via microscopy and flow cytometry.

Reporter System Quantifies Vomocytosis Rates of CN after Phagocyte Infection

Next, the ability of the reporter system to measure vomocytosis events was assessed. Cultures of MΦs or DCs were infected with pre-labeled CN at a 2:1 CN:phagocyte ratio and stained with AF594-Strep after 2 h and AF488-Ab after 24 h. The phagocytes were lysed using sterile water, a NIR LiveDead stain was applied, and the fluorescence of each CN was evaluated using flow cytometry (Figure 3A). The gating strategy involved first selecting CFW positive (CN signal) and then AF594-Strep negative (internalized at t = 2 h), followed by AF488-Ab positive events (exocytosed). Finally, the dead CN was removed from the final vomocytosis statistic based on NIR LiveDead signal gating. (Figure 3B) This gating strategy displayed a clear vomocytosed population of CN, indicating that the reporter system could measure vomocytosis rates. This reporter staining was performed on CN-infected MΦ and DC cultures and compared to HK CN-infected and refrigerated (after phagocytosis) negative controls (Figure 3C,D). For both MΦ and DC infections, the live CN groups displayed significantly higher vomocytosis occurrence than the refrigerated control, which was also significantly higher than the HK-infected control. To test if the vomocytosis events were due to

https://doi.org/10.1021/cbmi.3c00050
Chem. Biomed. Imaging 2023, 1, 725−737

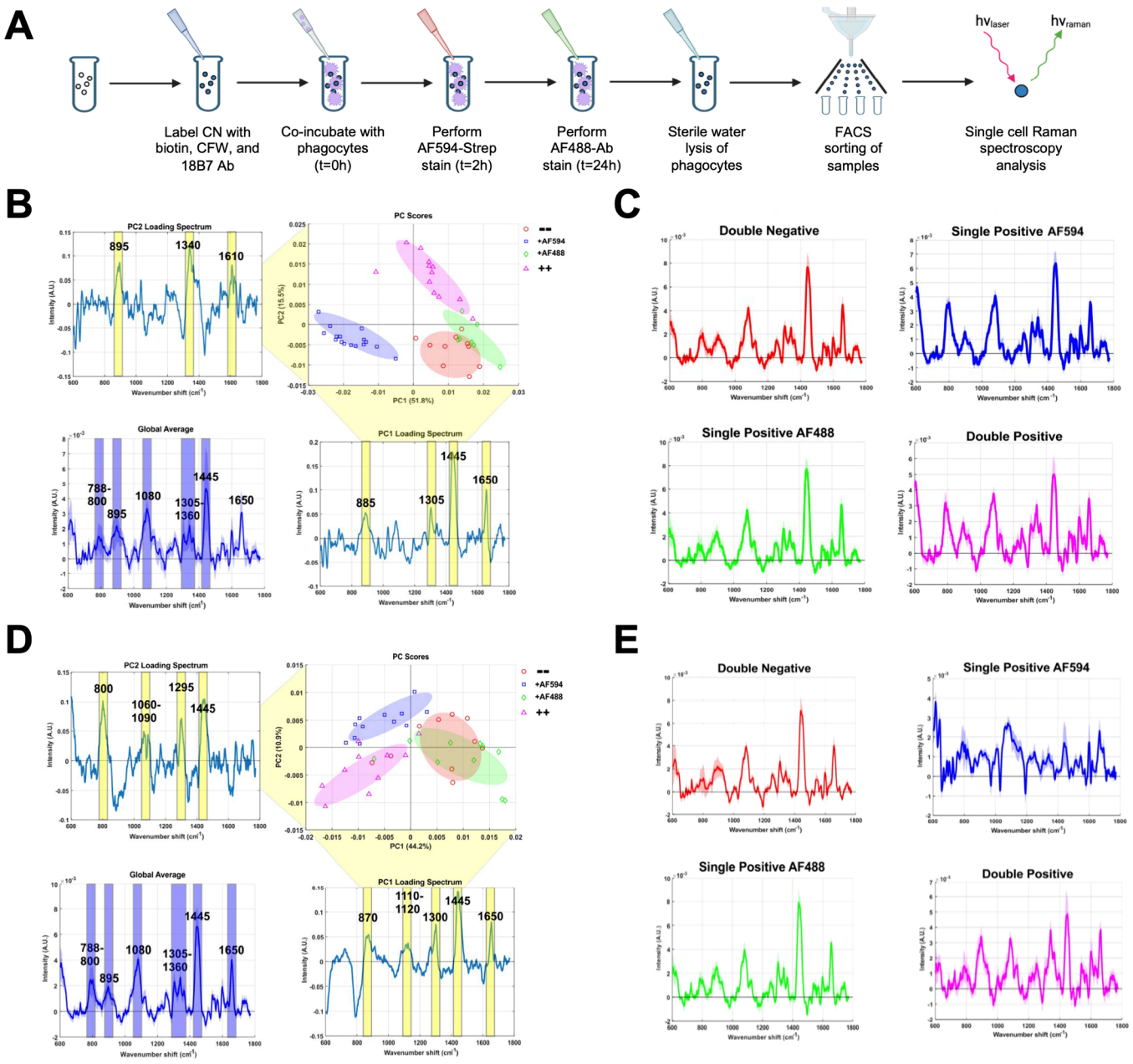

Figure 5. Single cell laser trapping Raman spectroscopy (LTRS) analysis of reporter-system-sorted CN after infection with MΦs or DCs. (A) Schematic outlining experimental design for Raman analysis of reporter-sorted CN. Like prior experiments, MΦs or DCs were infected with pre-labeled CN and stained with AF594-Strep and AF488-Ab during infection. After phagocyte lysis and NIR LiveDead staining, CN was sorted into 4 groups based on reporter fluorescent signals via FACS: double negative, single positive AF594-Strep, single positive AF488-Ab, and double positive groups. Multiple CNs ($n \geq 10$) were evaluated from each of the four populations via single cell LTRS for both MΦ infection and DC infection cultures. (B) Principal component analysis of reporter-sorted CN from DC infection. PCA plot displays clustering and separation of the 4 reporter-sorted CN groups (double negative, red circle, pre-strep internalization; single positive AF594-Strep, blue square, post-strep internalization; single positive AF488-Ab, green diamond, vomocytosis; double positive, purple triangle, no interaction). (C) Individual Raman fingerprints of reporter-sorted CN groups from DC infection. (D) Principal component analysis of reporter-sorted CN from MΦ infection. PCA plot displays clustering and separation of the 4 reporter-sorted CN groups. (E) Individual Raman fingerprints of reporter-sorted CN groups from MΦ infection.

phagocyte lysis during the experiment, the viability of MΦs and DCs during infection was assessed by PI staining and flow cytometric analysis. For both phagocyte types, the uninfected, live-infected, and HK-infected groups displayed minimal toxicity throughout a 24 h period compared to the dead control (Figure 3E,F). Overall, these data indicate that the reporter system can reliably measure vomocytosis events of CN-infected MΦs and DCs.

Reporter System Detects Differences in Vomocytosis Occurrence during Drug-Treated Conditions

It has been reported that vomocytosis involves the modulation of the phagosomal environment including pH[10,22−24] and disruption of the actin structure within the host phagocyte.[15] To further characterize the reporter system's ability to detect differences in vomocytosis rates, MΦs or DCs infected with CN were treated with phagosomal- and actin-modifying drugs (Figure 4A). The drugs used were CQ (a weak base known to

https://doi.org/10.1021/cbmi.3c00050
Chem. Biomed. Imaging 2023, 1, 725−737

increase phagosomal pH[25,26]), BFA (an ATPase inhibitor that prevents acidification and lysosome fusion in phagosomes[27,28]), or CYT (an inhibitor of actin polymerization and modulator of lysosomal fusion[29,30]) (Figure 4A). Cytochalasin B was used at two different concentrations of CYT hi (4 μM) or CYT lo (100 nM) due to the variable effects reported in the literature. In MΦ cultures, the CQ-treated group displayed a significantly reduced vomocytosis rate, while the BFA- and CYT hi-treated groups had higher expulsion occurrences (Figure 4B). For DCs infected with CN, the BFA and CYT hi groups also recorded higher incidences of vomocytosis measured by the reporter system (Figure 4C). Interestingly, the finding that CQ reduces MΦ vomocytosis rates conflicts with prior studies investigating J774 MΦ cell lines by Ma et al. and Nicola et al. but is in agreement with other observations in neutrophils and DCs.[2,7,8,10] The significant increase in vomocytosis rates in BFA-treated MΦ and DC infections differs from observations by Nicola et al. (in J774 MΦ) and Pacifici et al. (in primary DCs) that BFA treatment decreases expulsion rates.[8,10] All these findings differ from results reported by Yang et al., showing that neutrophil vomocytosis rates are unaffected by BFA treatment.[7] Lastly, the observed increase in vomocytosis rates for CYT hi-treated MΦ and DC groups aligns with previous studies investigating J774 MΦs by Alvarez et al.[1] and neutrophils by Yang et al.[7,10] However, again there exists disagreement within the literature, with decreases in CYT-modulated vomocytosis rates seen in J774 MΦs by Dragotakes et al. and DCs by Pacifici et al.[8,16] This inconsistency in prior studies may be due to the variety of cell types, cell sources, and vomocytosis measurement methodologies. Despite some differences compared to already conflicting literature, these findings indicate that the reporter system can measure differences in vomocytosis rates of drug-treated groups with high resolution and repeatability.

Reporter System Detects Differences in Pre-Filtered Expulsion and the Viability of Exocytosed CN

In measuring the vomocytosis rates using the reporter system, the dead CN was filtered out of the final calculation due to vomocytosis being defined as both the host and pathogen remaining alive. However, we still presented the total expelled CN (dead included) data in Figure S1A,C to gain further clarity on the interaction of these cells with MΦs and DCs. When analyzing the unfiltered expulsion events, the HK CN and refrigerated groups still displayed lower rates than the live CN group for both MΦ and DC infections, although the HK CN group showed a nonzero number of expulsions, unlike the vomocytosis statistics. For both CN-infected MΦs and DCs, the BFA and CYT hi groups displayed higher unfiltered expulsions than the live control. However, infected DCs showed higher CN expulsions in the CQ-treated group. Unlike the vomocytosis statistic, the CN-infected MΦ group treated with CQ did not see any significant difference from the control group (Figure S1A,C). In investigating the viability of expelled CN, the percentage of killed CN was observed to be significantly higher in the CQ-treated group for both MΦ and DC infections (Figure S1B,D). This is in-line with reports that CQ has some antifungal activity in phagocytes.[31−33] Interestingly, the CN-infected, DC refrigerated group displayed significantly higher % killed expelled CN compared to the control group, which indicates that potentially CN is sensitive to temperature combined with intraphagosomal conditions.

Reporter-Stained FACS-Sorted CN Groups Display Distinct Compositional Differences Measured by Single Cell Laser Trapping Raman Spectroscopy Analysis

The reporter system staining scheme can not only be used to measure vomocytosis rates via analytical flow cytometry but can also be used to sort reporter-stained populations via FACS for downstream analysis purposes. We aimed to characterize the biochemical composition of each reporter-stained CN population scenario for both infected DC and MΦ cultures using single cell laser trapping Raman spectroscopy (LTRS) analysis. To achieve this, reporter-stained CN-infected MΦ and DC cultures were FACS-sorted by AF594-Strep and AF488-Ab signal, resulting in 4 sorted CN populations for each phagocyte type. After FACS sorting, each population was assessed via flow cytometry showing high post-sort purity of 78% or higher (Figure S2). Raman spectroscopy has proven an ideal tool for biochemical characterization of a broad range of various samples types ranging from metabolites and other small molecules to extracellular vesicles and whole cell analyses.[20,34−36] In Raman spectroscopy, monochromatic photons from a laser irradiate the sample of interest, of which a small proportion are inelastically scattered with energies resultant of the molecules probed. Thus, an acquired Raman spectrum can be considered as a chemical fingerprint of the sample, wherein each spectral peak or band corresponds to certain chemical features, for example, the underling chemical bonds of nucleic acids or proteins. In this study, the sorted CN populations were analyzed via single cell LTRS[17−19] to produce a unique fingerprint to be used for comparison of the chemical composition of each group (Figure 5A). To the best of our knowledge, this is the first report of LTRS analysis of CN. For DCs and MΦs, each reporter-sorted population of CN displayed unique Raman properties. These differences are visualized via cluster separation within principal component analysis (PCA) plots and group average spectra for double negative, single positive AF594, single positive AF488, and double positive CN. PCA is a widely used multivariate analysis technique[37] to reduce the dimensionality of spectral data whereby the pertinent features contributing the most to differences between the sample groups can be discerned. This results in a PCA scores plot that displays each measured spectrum as a single marker in the plot, with each axis in the scores plot representing a corresponding loading spectrum containing the features that correspond to most of the variation within the given data set. For clarity, the global average spectra of CNs used to infect DCs and MΦs are shown in Figure 5 as well. Lastly, the average Raman spectra of each measured group is shown in Figure 5, panels C and E (Figure 5B−E). As represented in Figure 5B, there is a distinct separation between the different groups. The principal component (PC) 1 and 2 correspond to 51.8% and 15.5% of total variation within the data set and thus are presented here. In the PC scores plot and the associated PC1 loading spectrum, the double negative (red circles), AF488 single positive (green diamonds), and double positive (purple triangles) CNs express more carbohydrate-, protein-, and phospholipid-related vibrations than the AF594 single positive CNs (Table 1). Also, by analyzing the PC2 loading spectrum, the double positive CNs exhibit more carbohydrate- and protein-associated spectral features than the three other CN groups. Although currently beyond the scope of this study, we hypothesize that especially the surface structures of CNs undergo chemical changes during the phagocytosis/vomocy-

https://doi.org/10.1021/cbmi.3c00050
Chem. Biomed. Imaging 2023, 1, 725−737

Table 1. Raman Spectra Peak/Band Assignments

Peak/Band	Chemical Assignment
788−800	Nucleic acid vibrations[19]
870	Carbohydrate-related vibrations[19]
885	Carbohydrate-related vibrations[19]
895	Carbohydrate-related vibrations[19]
1060−1090	Majorly lipid vibrations[19,20]
1080	Majorly lipid vibrations[19,20]
1110−1120	C−C vibrations in, e.g., lipids; C−N amide vibrations in proteins[19]
1295	Protein (amide III)/phospholipid vibrations[38]
1300	Protein (amide III)/ phospholipid vibrations[38]
1305−1360	Protein (amide III)/ phospholipid vibrations[38]
1445	CH_2 and CH_3 deformations in proteins and lipids[18]
1610	Protein vibrations[39]
1650	Amide I vibrations is proteins or C=C stretching in lipids[19]

tosis processes, while the double negative CNs (i.e., no interaction with the phagocytes) remain unchanged. Intriguingly, the CNs that have interacted with MΦs (Figure 5D) show a slightly different trend. By first inspecting the PC scores plot with the PC1 loading spectrum, the double negative and AF488 single positive CNs express more carbohydrate-, protein-, and phospholipid-associated spectral features than the AF594 single negative and double positive CNs. Moving forward to the interpretation of the PC2 loading spectrum, especially the AF594 single positive group has more of these chemical features than the rest. However, since PC1 corresponds to 44.2% and PC2 to 10.9% of total variation within this data set, it yields the predominant interpretation of the spectral data of CNs that have interacted with MΦs. Careful to avoid overinterpretation of this Raman spectral data, we hypothesize that these clear differences—not only within the sample groups but also between the CNs that had interacted with DCs and MΦs—likely report on the chemical modification the CNs undergo during the phagocytosis/vomocytosis cycles. Interestingly, there is some overlap between double negative CN (pre-strep internalization) and single AF488-Ab positive (vomocytosis) groups on the PCA plot for MΦs (Figure 5D). This result can be justified since pre-strep internalization is the step prior to vomocytosis, and CN can in this case experience biochemical modification that results in similar expression of these molecular markers. Lastly, a similar pattern can also be seen in the LTRS results of CNs that have interacted with DC (Figure 5B). Although not clearly overlapping, the double negative and AF488 single positive groups are close to each other there as well. Taken together, this investigation demonstrates that (1) the reporter system can be used to successfully analyze vomocytosed populations for downstream processes and (2) different reporter-stained CN populations have distinct molecular signatures that can be measured by Raman spectroscopy.

Modified Reporter System Measures Pseudo Vomocytosis Rates of PLGA MPs

Currently, there exist no methods to accurately measure exocytosis of biomaterial particulates. To test the application potential of the reporter system, and to fulfill the need for a method to measure expulsion of particles, we translated the reporter staining scheme to PLGA MPs. Polymeric PLGA MPs were chosen due to their wide usage as a biodegradable biomaterial drug delivery platform with tunable size, chemistry, and release kinetics properties.[40] The key changes to the reporter system for PLGA MPs included replacing the CFW tracker dye with FITC, conjugated via click chemistry. Additionally, the biotin was conjugated to the surface of the PLGA MPs via click chemistry. The fluorescent antibody used for this system was an allophycocyanin (APC) conjugate of an anti-FITC antibody (APC-Ab) targeting the conjugated tracker FITC dye (Figure 6A). These alterations were necessary to account for the differences in surface properties of fungal cells and PLGA MPs. To confirm that each reporter component functioned properly, pre-labeled PLGA MPs were incubated with MΦs to allow for phagocytosis and subsequently stained with reporter components. Fluorescence microscopy was used to visualize FITC tracker (blue), AF594-Strep (red), and APC-Ab (green) signal. The pre-labeled FITC tracker displayed a clear signal on all PLGA MPs. On the other hand, the AF594-Strep and APC-Ab signals distinctly labeled only extracellular MPs, clearly displaying successful selective staining (Figure 6B). Additionally, flow cytometry of lysed cultures displayed clearly gated populations based on AF594-Strep or APC-Ab signal to determine the location of the particle (Figure 6C). These results indicate that the modified reporter system components act as expected with high resolution and selective staining. Next, this system was tested for its ability to detect expulsion events of PLGA MPs. Biomaterial particles do not inherently perform vomocytosis. Therefore, water was used to lyse open phagocytes to imitate expulsion in order to test the reporter system in PLGA MPs (Figure 6D). Compared to an unlysed control, the partially lysed PLGA MP treatment group displayed a significantly higher expulsion rate readout using this reporter system for both MΦ and DC phagocyte types (Figure 6E,F). Taken together, these data strongly support the potential of this reporter system to measure vomocytosis rates of PLGA MPs from phagocytes and suggest that the system can likely be universally implemented for numerous different pathogens and particles.

4. CONCLUSION

This study characterizes a facile, reporter staining scheme primarily consisting of two extracellular staining steps during phagocyte infection, followed by flow cytometry analysis. The AF594-Strep and AF488-Ab stains were verified to selectively stain CN located outside of the phagosome through fluorescence microscopy, flow cytometry, and confocal microscopy. Furthermore, this system was verified to successfully detect real vomocytosis events of CN from both MΦ and DC infections. This approach has the ability to resolve significant differences in expulsion rates of drug treatments affecting phagosomal and actin machinery. Through FACS sorting and single cell laser trapping Raman spectroscopy analysis, different reporter-stained CN populations exhibited unique chemical compositions, indicating differences in biological expression of CN under different phagocyte interaction outcomes. Finally, this reporter methodology was adapted to properly function on biologically inert PLGA MPs to measure pseudo vomocytosis events from partially lysed phagocyte cultures incubated with these particles.

In conclusion, the reporter system we developed is proven to be a simple, high-throughput method to measure vomocytosis with minimal labor and maximal accuracy, while only requiring easily accessible resources and equipment. Furthermore, unlike any pre-existing methods, this reporter system can be used to

https://doi.org/10.1021/cbmi.3c00050
Chem. Biomed. Imaging 2023, 1, 725−737

A

	Tracking Label	Target 1	Extracellular Stain for Target 1	Target 2	Extracellular Stain for Target 2
C. neoformans	CFW	Biotin	AF594-Strep	18B7 Ab	AF488-Ab
PLGA MPs	FITC	Biotin	AF594-Strep	FITC	APC-Ab

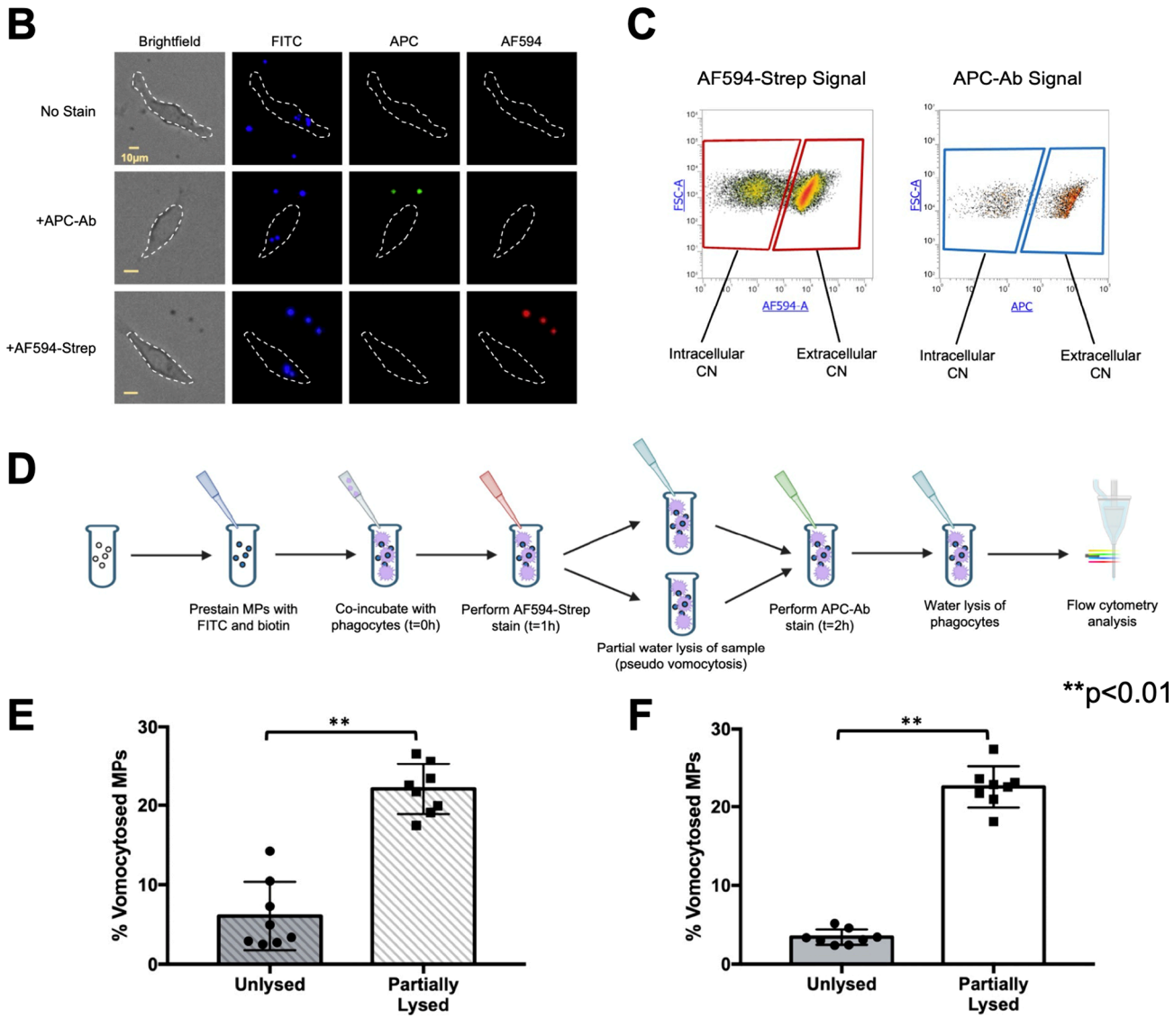

Figure 6. Translation of reporter system to biomaterial PLGA MPs and measurement of pseudovomocytosis rates. (A) Comparison of reporter system staining scheme for PLGA MPs compared to CN. The primary modifications were changing the tracking label from CFW to FITC and switching the AF488-Ab to an APC-Ab that targets FITC. Otherwise, the two designs have the same overall fundamental mechanism with a tracker dye and two extracellular stains during infection. (B) Fluorescence microscopy confirmation of extracellular staining ability of AF594-Strep and APC-Ab. The particle tracker FITC, shown in blue, is labeled on all PLGA MPs. When AF594-Strep staining (shown in red) is applied, only extracellular particles display a signal. If APC-Ab staining (shown in green) is performed, again only extracellular particles display a signal. (C) Flow cytometry confirmation of extracellular staining. After either AF594-Strep or APC-Ab staining, both lysed cultures displayed distinct gate-able flow cytometry populations by the respective fluorescence signal. (D) Experimental design schematic for measuring pseudovomocytosis rates of PLGA MPs. After PLGA MPs labeling with biotin and FITC, particles were incubated with MΦs or DCs for 1 h to allow for phagocytosis. Subsequently, a AF594-Strep stain was performed on the culture. To simulate vomocytosis, the tube was then split, and sterile water lysis was performed on half of the culture. Finally, the APC-Ab stain was performed, cultures were fully lysed using water, and PLGA MPs were analyzed via flow cytometry. (E) Bar graph showing pseudovomocytosis rates of PLGA MPs when co-incubated with MΦ cultures. Rates are shown for both unlysed and partially lysed conditions ($N = 3$, $n = 8$). (F) Bar graph showing pseudovomocytosis rates of PLGA MPs when co-incubated with DC cultures. Rates are shown for both unlysed and partially lysed conditions ($N = 3$, $n = 8$). All statistical analyses were unpaired t tests performed via GraphPad Prism 9.

https://doi.org/10.1021/cbmi.3c00050
Chem. Biomed. Imaging 2023, 1, 725−737

detect expulsion events in biomaterial PLGA MPs. One limitation of this reporter system is that replication of CN may affect reporter gating percentages, especially since the number of expelled CN is counted rather than the number of vomocytic cells (vomocytes). However, the impact of fungal replication is minimized by usage of a *Cdc24* mutant strain that inhibits replication at 37 °C during the infection and CFW gating that prioritizes parent CN during analysis.

Our improved methodology for studying vomocytosis opens the door for high throughput screening of drug treatments and knockout libraries. Additionally, there is high potential for improved resolution for downstream analyses including proteomics and single cell RNaseq of CN after reporter staining and sorting. By contributing this powerful tool to the arsenal of vomocytosis research, we hope that it will boost new high impact discoveries in this promising field of study, helping to reveal more about the underlying mechanisms of this fascinating mechanism and pathogen.

■ ASSOCIATED CONTENT

Supporting Information

The Supporting Information is available free of charge at https://pubs.acs.org/doi/10.1021/cbmi.3c00050.

Statistically significant comparisons from all figures; expulsion rates and viability percentages used to calculate vomocytosis rates; pre-sort and post-sort purity of reporter-stained CN (PDF)

■ AUTHOR INFORMATION

Corresponding Author

Jamal S. Lewis − *Department of Biomedical Engineering, University of California-Davis, Davis, California 95616, United States; J. Crayton Pruitt Family Department of Biomedical Engineering, University of Florida, Gainesville, Florida 32611, United States;* orcid.org/0000-0002-9811-8538; Email: JLewis@bme.ufl.edu

Authors

Noah Pacifici − *Department of Biomedical Engineering, University of California-Davis, Davis, California 95616, United States*

Tatu Rojalin − *Department of Biomedical Engineering, University of California-Davis, Davis, California 95616, United States;* orcid.org/0000-0002-9805-1353

Randy P. Carney − *Department of Biomedical Engineering, University of California-Davis, Davis, California 95616, United States;* orcid.org/0000-0001-8193-1664

Complete contact information is available at: https://pubs.acs.org/10.1021/cbmi.3c00050

Notes

The authors declare no competing financial interest.

■ ACKNOWLEDGMENTS

The authors thank Dr. Arturo Casadevall and Dr. Maggie Wear for their generous gift of 18B7 antibody. We are grateful to the Gelli Lab at UC Davis for providing the CN strains used in this study. Additionally, we thank the George Lab at UC Davis for graciously allowing us to use their confocal equipment and aiding in performing confocal imaging. We acknowledge support from the following sources: NIH Grant R01AI139399 (J.S.L.), NIH Grant R35GM125012 (J.S.L.), NIH Grant R01CA241666 (R.P.C.), NIGMS-funded Pharmacology Training Program Grant T32GM099608 (N.P.), and NSF GRFP Grant 1650042 (N.P.).

■ REFERENCES

(1) Alvarez, M.; Casadevall, A. Phagosome Extrusion and Host-Cell Survival after Cryptococcus Neoformans Phagocytosis by Macrophages. *Curr. Biol.* **2006**, *16* (21), 2161−2165.

(2) Ma, H.; Croudace, J. E.; Lammas, D. A.; May, R. C. Expulsion of Live Pathogenic Yeast by Macrophages. *Curr. Biol.* **2006**, *16* (21), 2156−2160.

(3) Cruz-Acuña, M.; Pacifici, N.; Lewis, J. S. Vomocytosis: Too Much Booze, Base, or Calcium? *mBio* **2019**, DOI: 10.1128/mBio.02526-19.

(4) Seoane, P. I.; May, R. C. Vomocytosis: What We Know so Far. *Cell Microbiol* **2020**, *22* (2), No. e13145.

(5) May, R. C.; Stone, N. R. H.; Wiesner, D. L.; Bicanic, T.; Nielsen, K. Cryptococcus: From Environmental Saprophyte to Global Pathogen. *Nat. Rev. Microbiol* **2016**, *14* (2), 106−117.

(6) Rajasingham, R.; Smith, R. M.; Park, B. J.; Jarvis, J. N.; Govender, N. P.; Chiller, T. M.; Denning, D. W.; Loyse, A.; Boulware, D. R. Global Burden of Disease of HIV-Associated Cryptococcal Meningitis: An Updated Analysis. *Lancet Infectious Diseases* **2017**, *17* (8), 873−881.

(7) Yang, X.; Wang, H.; Hu, F.; Chen, X.; Zhang, M. Nonlytic Exocytosis of Cryptococcus Neoformans from Neutrophils in the Brain Vasculature. *Cell Communication and Signaling* **2019**, *17* (1), 117.

(8) Pacifici, N.; Cruz-Acuña, M.; Diener, A.; Tu, A.; Senthil, N.; Han, H.; Lewis, J. S. Vomocytosis of Cryptococcus Neoformans Cells from Murine, Bone Marrow-Derived Dendritic Cells. *PLoS One* **2023**, *18* (3), No. e0280692.

(9) Huth, J.; Buchholz, M.; Kraus, J. M.; Schmucker, M.; von Wichert, G.; Krndija, D.; Seufferlein, T.; Gress, T. M.; Kestler, H. A. Significantly Improved Precision of Cell Migration Analysis in Time-Lapse Video Microscopy through Use of a Fully Automated Tracking System. *BMC Cell Biol.* **2010**, *11*, 24.

(10) Nicola, A. M.; Robertson, E. J.; Albuquerque, P.; Derengowski, L. d. S.; Casadevall, A. Nonlytic Exocytosis of Cryptococcus Neoformans from Macrophages Occurs In Vivo and Is Influenced by Phagosomal PH. *mBio* **2011**, DOI: 10.1128/mBio.00167-11.

(11) Frazao, S. d. O.; Sousa, H. R. d.; Silva, L. G. d.; Folha, J. d. S.; Gorgonha, K. C. d. M.; Oliveira, G. P. d.; Felipe, M. S. S.; Silva-Pereira, I.; Casadevall, A.; Nicola, A. M.; Albuquerque, P. Laccase Affects the Rate of Cryptococcus Neoformans Nonlytic Exocytosis from Macrophages. *mBio* **2020**, *11* (5), e02085−20.

(12) Nicola, A. M.; Albuquerque, P.; Martinez, L. R.; Dal-Rosso, R. A.; Saylor, C.; De Jesus, M.; Nosanchuk, J. D.; Casadevall, A. Macrophage Autophagy in Immunity to Cryptococcus Neoformans and Candida Albicans. *Infect. Immun.* **2012**, *80* (9), 3065−3076.

(13) Allen, R. P.; Bolandparvaz, A.; Ma, J. A.; Manickam, V. A.; Lewis, J. S. Latent, Immunosuppressive Nature of Poly(Lactic-Co-Glycolic Acid) Microparticles. *ACS Biomater. Sci. Eng.* **2018**, *4* (3), 900−918.

(14) Nichols, C. B.; Perfect, Z. H.; Alspaugh, J. A. A Ras1-Cdc24 Signal Transduction Pathway Mediates Thermotolerance in the Fungal Pathogen Cryptococcus Neoformans. *Mol. Microbiol.* **2007**, *63* (4), 1118−1130.

(15) Johnston, S. A.; May, R. C. The Human Fungal Pathogen Cryptococcus Neoformans Escapes Macrophages by a Phagosome Emptying Mechanism That Is Inhibited by Arp2/3 Complex-Mediated Actin Polymerisation. *PLOS Pathogens* **2010**, *6* (8), No. e1001041.

(16) Dragotakes, Q.; Fu, M. S.; Casadevall, A. Dragotcytosis: Elucidation of the Mechanism for Cryptococcus Neoformans Macrophage-to-Macrophage Transfer. *J. Immunol.* **2019**, *202*, 2661.

(17) Ashkin, A.; Dziedzic, J. M.; Bjorkholm, J. E.; Chu, S. Observation of a Single-Beam Gradient Force Optical Trap for Dielectric Particles. *Opt. Lett., OL* **1986**, *11* (5), 288−290.
(18) Smith, Z. J.; Lee, C.; Rojalin, T.; Carney, R. P.; Hazari, S.; Knudson, A.; Lam, K.; Saari, H.; Ibañez, E. L.; Viitala, T.; Laaksonen, T.; Yliperttula, M.; Wachsmann-Hogiu, S. Single Exosome Study Reveals Subpopulations Distributed among Cell Lines with Variability Related to Membrane Content. *Journal of Extracellular Vesicles* **2015**, *4* (1), 28533.
(19) Shipp, D. W.; Sinjab, F.; Notingher, I. Raman Spectroscopy: Techniques and Applications in the Life Sciences. *Adv. Opt. Photon., AOP* **2017**, *9* (2), 315−428.
(20) Rojalin, T.; Koster, H. J.; Liu, J.; Mizenko, R. R.; Tran, D.; Wachsmann-Hogiu, S.; Carney, R. P. Hybrid Nanoplasmonic Porous Biomaterial Scaffold for Liquid Biopsy Diagnostics Using Extracellular Vesicles. *ACS Sens.* **2020**, *5* (9), 2820−2833.
(21) Koster, H. J.; Rojalin, T.; Powell, A.; Pham, D.; Mizenko, R. R.; Birkeland, A. C.; Carney, R. P. Surface Enhanced Raman Scattering of Extracellular Vesicles for Cancer Diagnostics despite Isolation Dependent Lipoprotein Contamination. *Nanoscale* **2021**, *13* (35), 14760−14776.
(22) Fu, M. S.; Coelho, C.; De Leon-Rodriguez, C. M.; Rossi, D. C. P.; Camacho, E.; Jung, E. H.; Kulkarni, M.; Casadevall, A. Cryptococcus Neoformans Urease Affects the Outcome of Intracellular Pathogenesis by Modulating Phagolysosomal PH. *PLOS Pathogens* **2018**, *14* (6), No. e1007144.
(23) Smith, L. M.; Dixon, E. F.; May, R. C. The Fungal Pathogen Cryptococcus Neoformans Manipulates Macrophage Phagosome Maturation. *Cellular Microbiology* **2015**, *17* (5), 702−713.
(24) De Leon-Rodriguez, C. M.; Fu, M. S.; Corbali, M. O.; Cordero, R. J. B.; Casadevall, A. The Capsule of Cryptococcus Neoformans Modulates Phagosomal PH through Its Acid-Base Properties. *mSphere* **2018**, 3 (5). DOI: 10.1128/mSphere.00437-18
(25) Halcrow, P. W.; Geiger, J. D.; Chen, X. Overcoming Chemoresistance: Altering PH of Cellular Compartments by Chloroquine and Hydroxychloroquine. *Frontiers in Cell and Developmental Biology* **2021**, *9*, 170.
(26) Xia, M.-C.; Cai, L.; Zhang, S.; Zhang, X. A Cell-Penetrating Ratiometric Probe for Simultaneous Measurement of Lysosomal and Cytosolic PH Change. *Talanta* **2018**, *178*, 355−361.
(27) Tapper, H.; Sundler, R. Bafilomycin A1 Inhibits Lysosomal, Phagosomal, and Plasma Membrane H+-ATPase and Induces Lysosomal Enzyme Secretion in Macrophages. *Journal of cellular physiology* **1995**, *163* (1), 137−144.
(28) Klionsky, D. J.; Elazar, Z.; Seglen, P. O.; Rubinsztein, D. C. Does Bafilomycin A1 Block the Fusion of Autophagosomes with Lysosomes? *Autophagy* **2008**, *4* (7), 849−850.
(29) Zurier, R. B.; Hoffstein, S.; Weissmann, G. Cytochalasin B: Effect on Lysosomal Enzyme Release from Human Leukocytes. *Proc. Natl. Acad. Sci. U. S. A.* **1973**, *70* (3), 844−848.
(30) Koza, E. P.; Wright, T. E.; Becker, E. L. Lysosomal Enzyme Secretion and Volume Contraction Induced in Neutrophils by Cytochalasin B, Chemotactic Factor and A23187. *Proceedings of the Society for Experimental Biology and Medicine* **1975**, *149* (2), 476−479.
(31) Li, Y.; Wan, Z.; Liu, W.; Li, R. Synergistic Activity of Chloroquine with Fluconazole against Fluconazole-Resistant Isolates of Candida Species. *Antimicrob. Agents Chemother.* **2015**, *59* (2), 1365−1369.
(32) Levitz, S. M.; Harrison, T. S.; Tabuni, A.; Liu, X. Chloroquine Induces Human Mononuclear Phagocytes to Inhibit and Kill Cryptococcus Neoformans by a Mechanism Independent of Iron Deprivation. *J. Clin Invest* **1997**, *100* (6), 1640−1646.
(33) Harrison, T. S.; Griffin, G. E.; Levitz, S. M. Conditional Lethality of the Diprotic Weak Bases Chloroquine and Quinacrine against Cryptococcus Neoformans. *Journal of Infectious Diseases* **2000**, *182* (1), 283−289.
(34) Jarvis, R. M.; Goodacre, R. Discrimination of Bacteria Using Surface-Enhanced Raman Spectroscopy. *Anal. Chem.* **2004**, *76* (1), 40−47.
(35) Maquelin, K.; Kirschner, C.; Choo-Smith, L.-P.; van den Braak, N.; Endtz, H. P.; Naumann, D.; Puppels, G. J. Identification of Medically Relevant Microorganisms by Vibrational Spectroscopy. *J. Microbiol Methods* **2002**, *51* (3), 255−271.
(36) Butler, H. J.; Ashton, L.; Bird, B.; Cinque, G.; Curtis, K.; Dorney, J.; Esmonde-White, K.; Fullwood, N. J.; Gardner, B.; Martin-Hirsch, P. L.; Walsh, M. J.; McAinsh, M. R.; Stone, N.; Martin, F. L. Using Raman Spectroscopy to Characterize Biological Materials. *Nat. Protoc* **2016**, *11* (4), 664−687.
(37) Abdi, H.; Williams, L. J. Principal Component Analysis. *WIREs Computational Statistics* **2010**, *2* (4), 433−459.
(38) Xie, C.; Chen, D.; Li, Y. Raman Sorting and Identification of Single Living Micro-Organisms with Optical Tweezers. *Opt. Lett., OL* **2005**, *30* (14), 1800−1802.
(39) Kengne-Momo, R. P.; Daniel, P.; Lagarde, F.; Jeyachandran, Y. L.; Pilard, J. F.; Durand-Thouand, M. J.; Thouand, G. Protein Interactions Investigated by the Raman Spectroscopy for Biosensor Applications. *International Journal of Spectroscopy* **2012**, *2012*, No. e462901.
(40) Makadia, H. K.; Siegel, S. J. Poly Lactic-Co-Glycolic Acid (PLGA) as Biodegradable Controlled Drug Delivery Carrier. *Polymers (Basel)* **2011**, *3* (3), 1377−1397.